Electronic Supplementary Material (ESI) for Soft Matter.

Cholesterol in phospholipid bilayers: positions and orientations inside membranes with different unsaturation degree

Supplementary Information

Inna Ermilova, Alexander P. Lyubartsev

Department of Materials and Environmental Chemistry,
Stockholm University, SE 106 91, Stockholm, Sweden

Content

- Figure S1: Order parameters for sn-1 and sn-2 chains of lipids in pure and cholesterol-containing bilayers.
- Figures S2-S7: Mass density and electron density profiles for some bilayers
- Figures S8-S14: Various RDFs between cholesterol and lipids atoms
- Figures S15-S16: Two-dimensional density maps illustrating location and orientation of cholesterol in some lipid bilayers
- Figure S17: Two-dimensional free energy maps illustrating location and orientation of cholesterol in some lipid bilayers
- Figure S18-S19: One-dimensional free energy profiles along the membrane normal and as a function of cholesterol orientation
- Figures S20-S26: Analysis of convergence of Metadynamics simulations

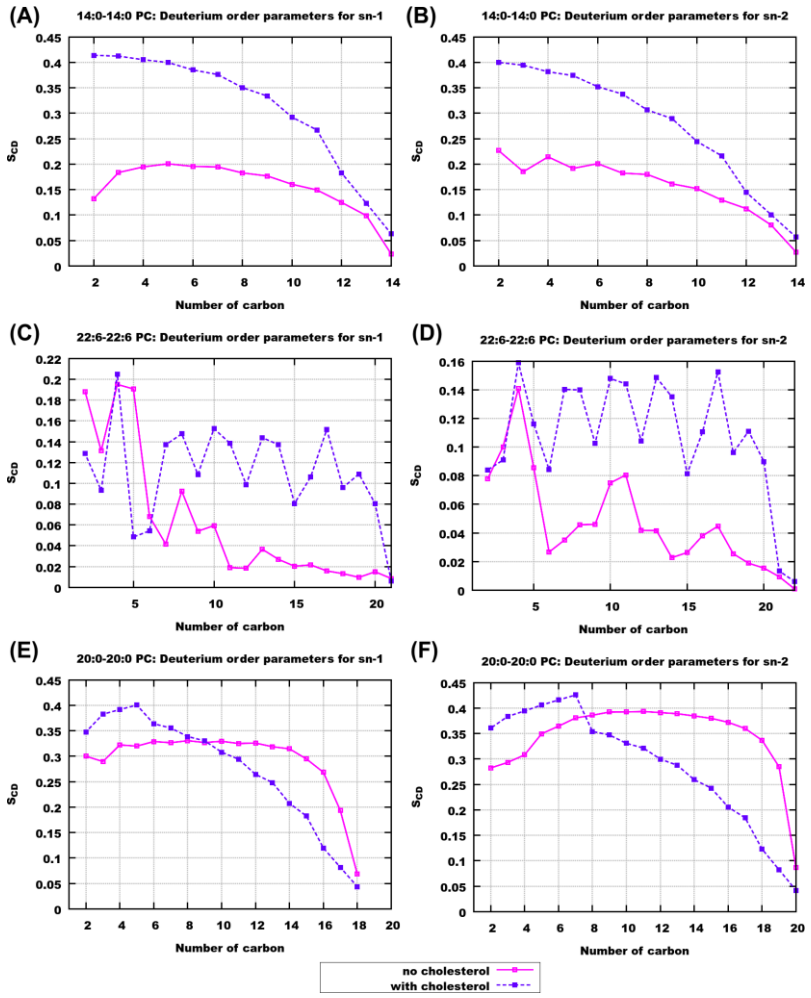

Figure S1: Order parameters for sn-1 and sn-2 chains of lipids in pure and 50 % cholesterol-containing bilayers: 14:0-14:0 PC (A,B), 22:6-22:6 PC (C,D) and 20:6-20:6 PC (E.F). While for fully saturated liquid phase bilayer 14:0-14:0 PC and strongly unsaturated 22:6-22:6 PC bilayer the order parameters increase upon addition of cholesterol, for gel-phase 20:0-20:0 PC bilayer addition of cholesterol leads to noticeable decrease of the order parameters in the lower parts of acyl tails.

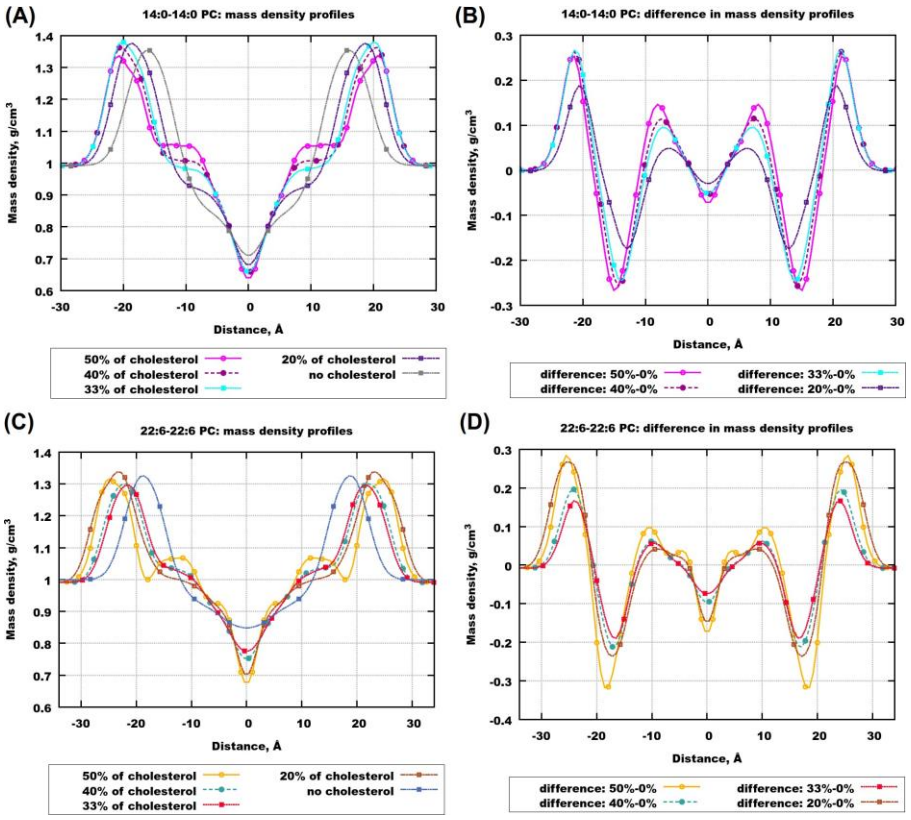

Figure S2: Mass density profiles for 14:0-14:0 PC and 22:6-22:6 PC with different concentrations of cholesterol. (A) Mass density profiles for 14:0-14:0 PC bilayers containing different amounts of cholesterol. (B) Difference in mass density profiles between 14:0-14:0 PC bilayer with cholesterol and pure bilayer. (C) Mass density profiles for 22:6-22:6 PC bilayers containing different amounts of cholesterol. (D) Difference in mass density profiles between 22:6-22:6 PC bilayer with cholesterol and pure bilayer.

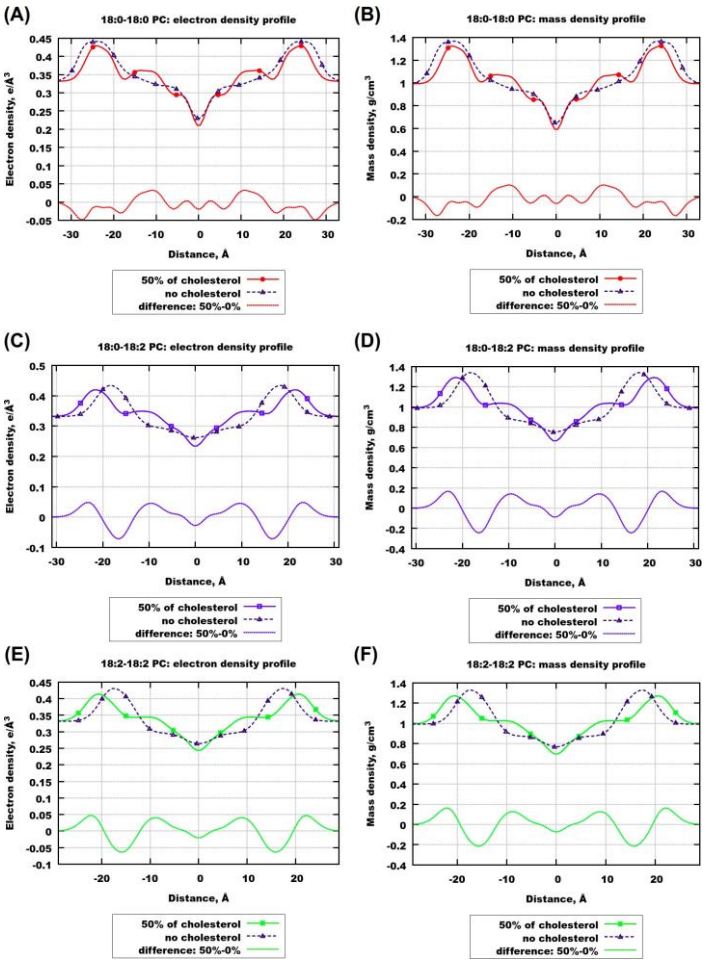

Figure S3: Electron density profiles and mass density profiles for selected lipid bilayers with 50 % *mol* of cholesterol (labelled as ”50 % of cholesterol”) and pure bilayers (labelled as ”no cholesterol”). Also shown is difference profile (labelled as ”difference: 50 % -0%”) which is a result of substraction of the profile without cholesterol from the profile with cholesterol.

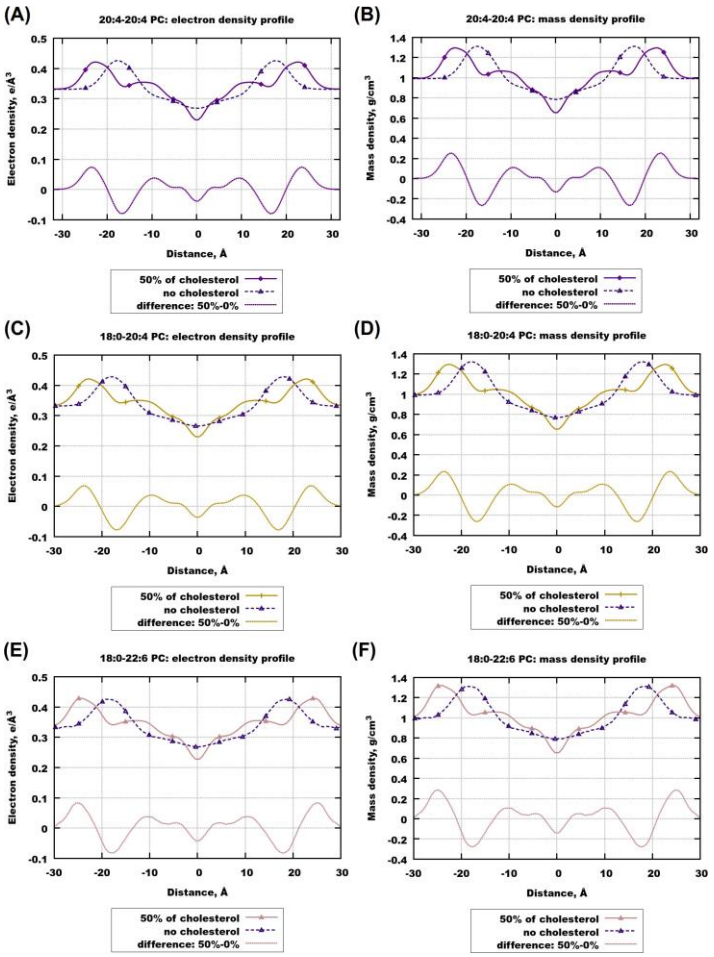

Figure S4: Electron density profiles and mass density profiles for selected lipid bilayers with 50 % *mol* of cholesterol (labelled as ”50 % of cholesterol”) and pure bilayers (labelled as ”no cholesterol”). Also shown is difference profile (labelled as ”difference: 50 % -0%”) which is a result of substraction of the profile without cholesterol from the profile with cholesterol.

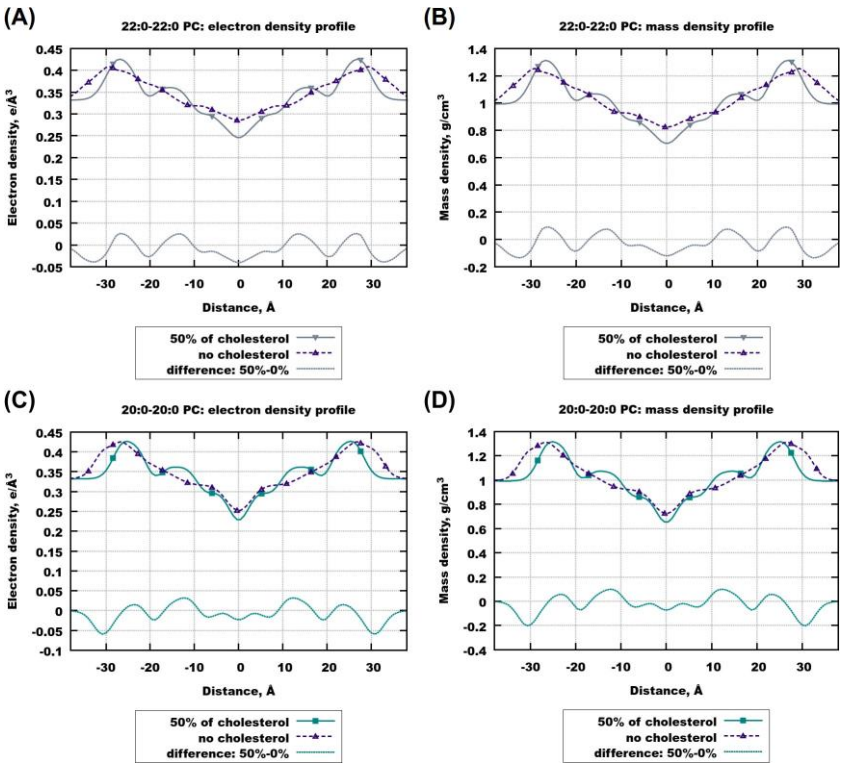

Figure S5: Electron density profiles and mass density profiles for selected lipid bilayers with 50 % *mol* of cholesterol (labelled as ”50 % of cholesterol”) and pure bilayers (labelled as ”no cholesterol”). Also shown is difference profile (labelled as ”difference: 50 % -0%”) which is a result of substraction of the profile without cholesterol from the profile with cholesterol.

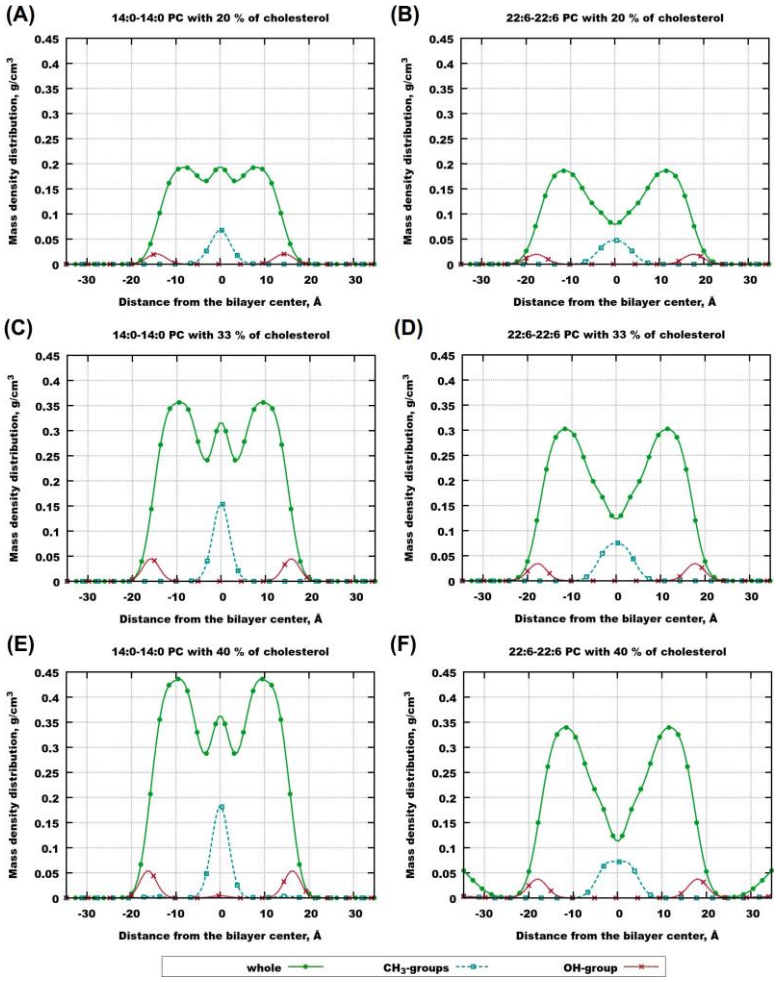

Figure S6: Contributions of cholesterol molecules to the electron density in selected bilayers. Here: "whole" is a contribution from the whole cholesterol molecule; "CH_3-groups" stands for the contribution from terminal CH_3-groups in the cholesterol tail; "*OH*-group" stands for the contribution from *OH* cholesterol group.

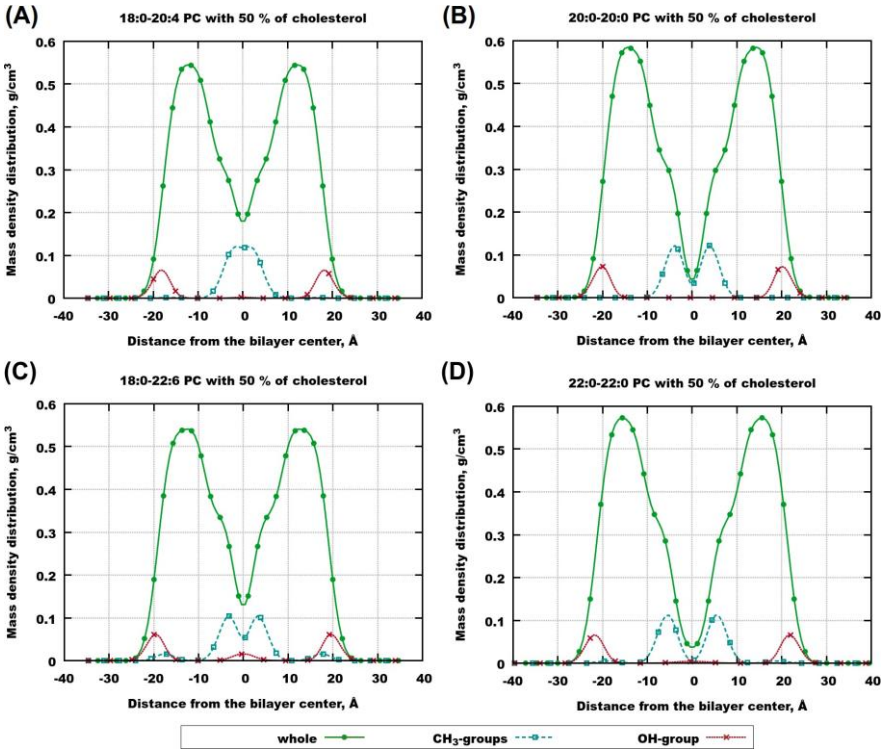

Figure S7: Contributions of cholesterol molecules to the electron density in selected bilayers. Here: "whole" is a contribution from the whole cholesterol molecule; "CH_3-groups" stands for the contribution from terminal CH_3-groups in the cholesterol tail; "*OH*-group" stands for the contribution from *OH* cholesterol group.

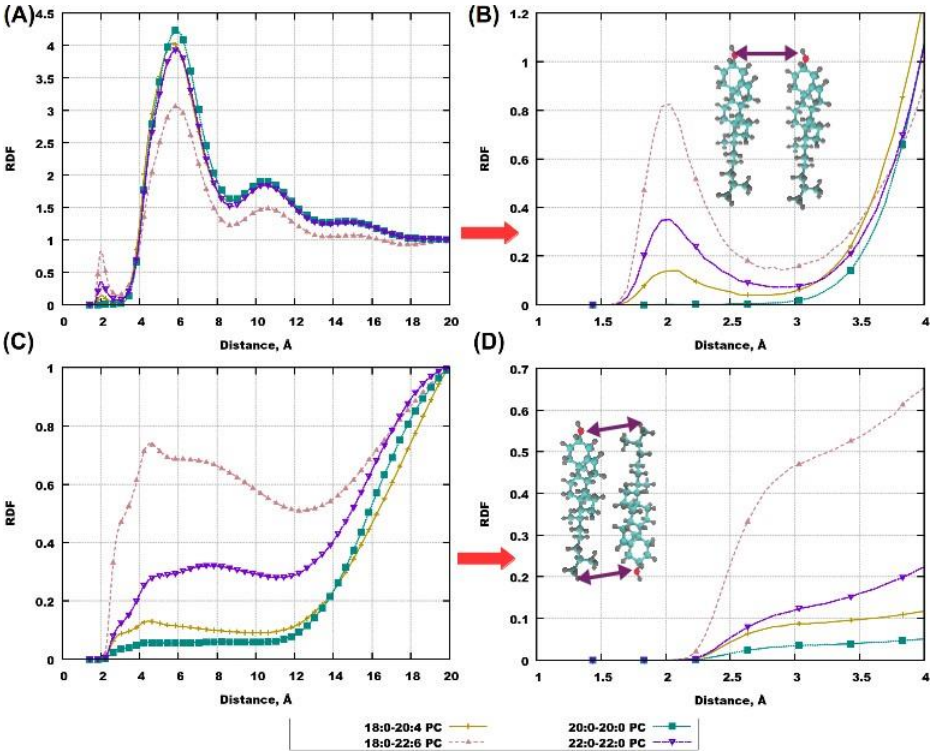

Figure S8: RDF between cholesterol molecules for selected bilayers with 50% cholesterol content. (A,B): RDF between oxygen of the hydroxyl group of cholesterol and hydrogen of the hydroxyl group of another cholesterol molecule. (C,D): RDF between oxygen of the hydroxyl group of cholesterol and hydrogen atoms in the terminal methyl group of another cholesterol molecule. (A,C): RDFs in the whole range of distances; (B,D): Same RDFs in a short range of distances.

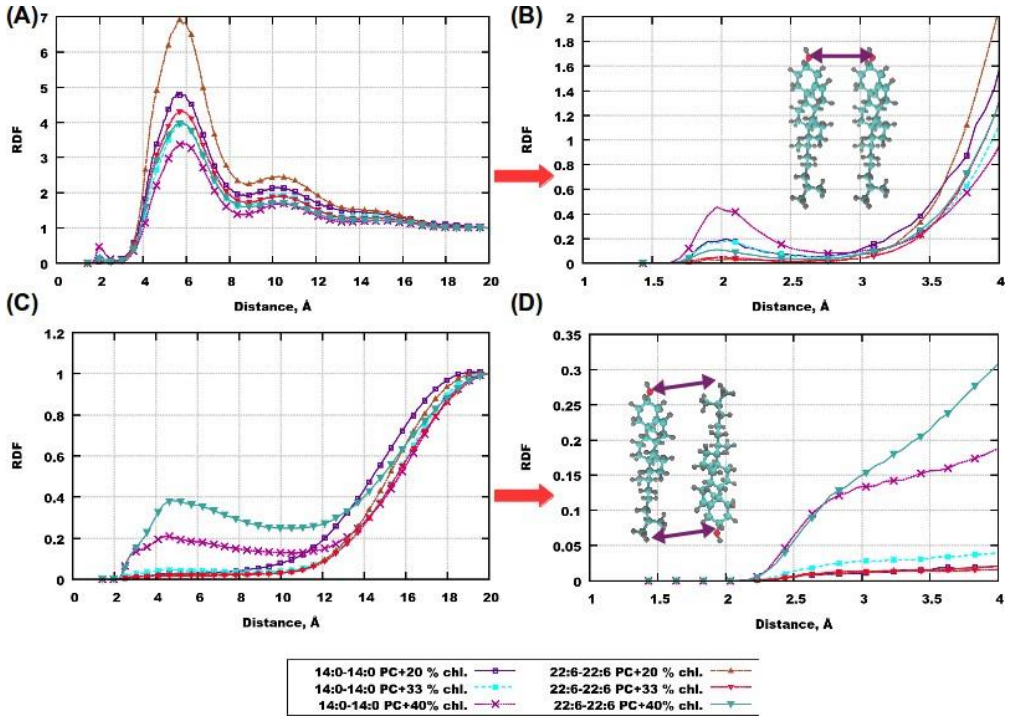

Figure S9: RDF between cholesterol molecules for 14:0-14:0 PC and 22:6-22:6 PC bilayers with varying cholesterol content. (A,B): RDF between oxygen of the hydroxyl group of cholesterol and hydrogen of the hydroxyl group of another cholesterol molecule. (C,D): RDF between oxygen of the hydroxyl group of cholesterol and hydrogen atoms in the terminal methyl group of another cholesterol molecule. (A,C): RDFs in the whole range of distances; (B,D): Same RDFs in a short range of distances.

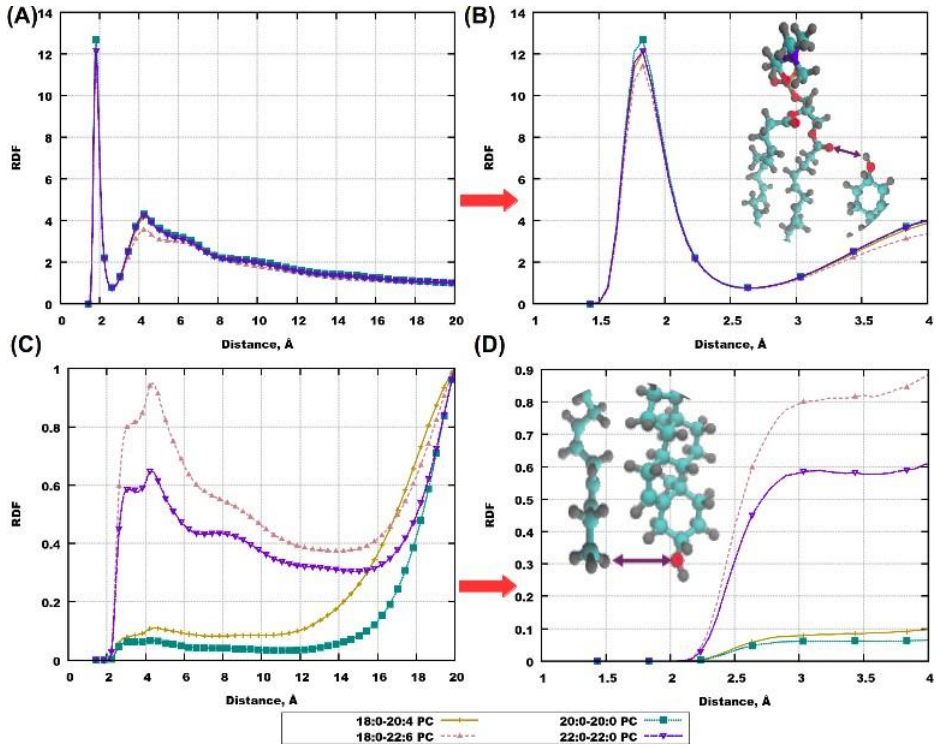

Figure S10: RDF between cholesterol molecules and lipids for selected bilayers with 50% cholesterol content. (A,B): RDF between oxygen of the cholesterol hydroxyl group and oxygen of the lipid ester group; (C.D): RDF between oxygen of the cholesterol hydroxyl group and hydrogen of the terminal methyl groups of lipid tails. (A,C): RDFs in the whole range of distances; (B,D): Same RDFs in a short range of distances.

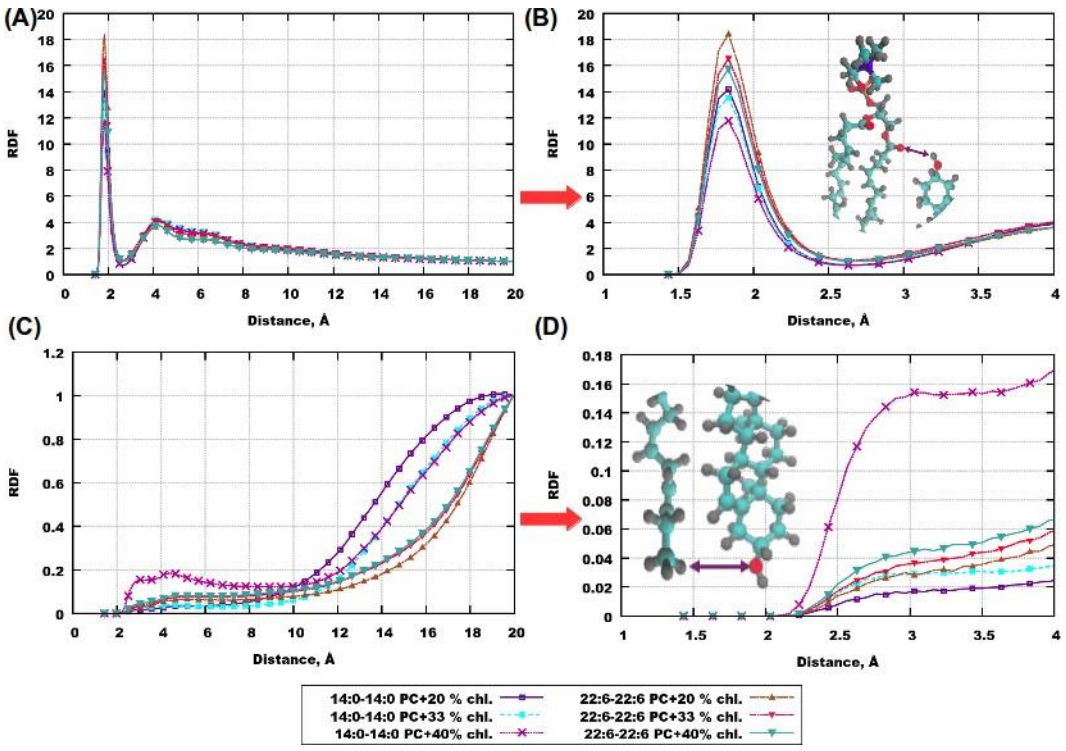

Figure S11: RDF between cholesterol molecules and lipids for 14:0-14:0 PC and 22:6-22:6 PC bilayers with varying cholesterol content. (A,B): RDF between oxygen of the cholesterol hydroxyl group and oxygen of the lipid ester group; (C.D): RDF between oxygen of the cholesterol hydroxyl group and hydrogen of the terminal methyl groups of lipid tails. (A,C): RDFs in the whole range of distances; (B,D): Same RDFs in a short range of distances.

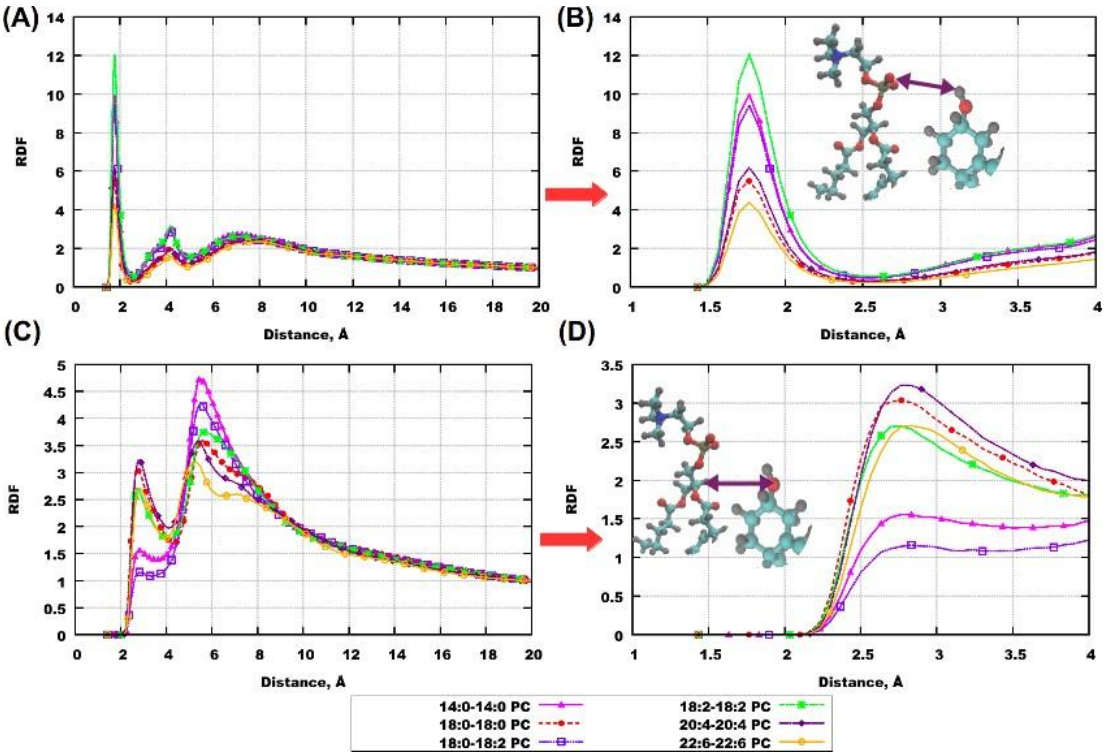

Figure S12: RDFs between cholesterol molecules and lipids for selected bilayers with 50% cholesterol content. (A,B) RDF between oxygen of the hydroxyl group of cholesterol molecules and oxygen of the phosphate group of lipid head; (C,D) RDF between oxygen of the hydroxyl group of cholesterol molecules and hydrogens of the *CH* group in the lipid glycerol fragment. (A,C): RDFs in the whole range of distances; (B,D): Same RDFs in a short range of distances.

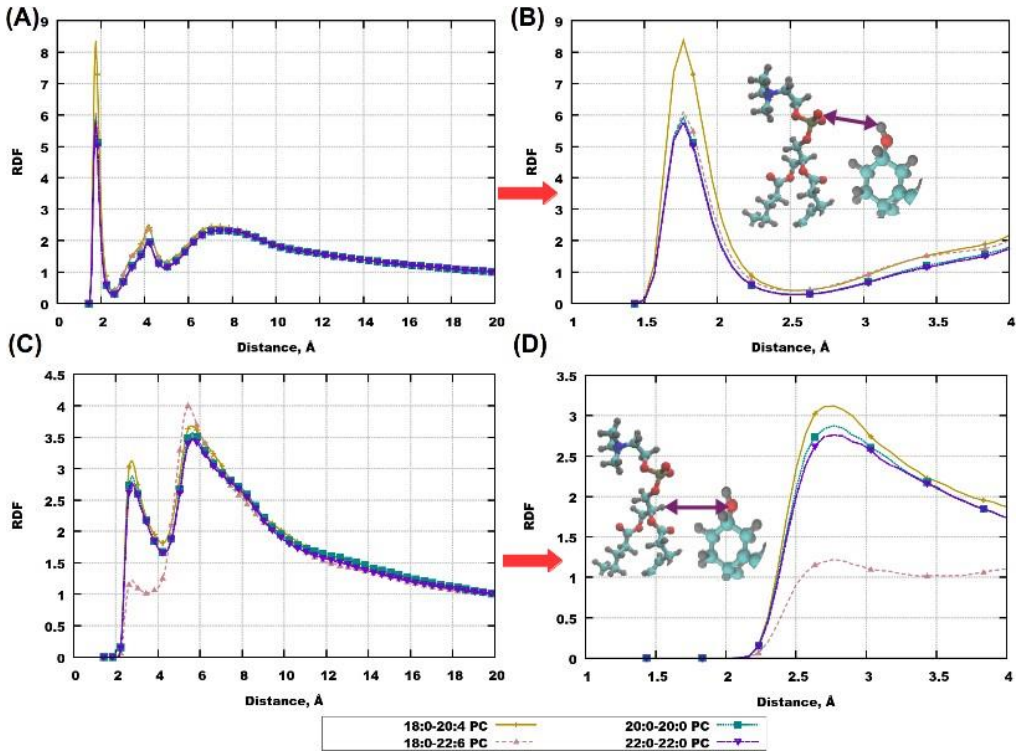

Figure S13: RDFs between cholesterol molecules and lipids for selected bilayers with 50% cholesterol content. (A,B): RDF between oxygen of the hydroxyl group of cholesterol molecules and oxygen of the phosphate group of lipid head; (C,D): RDF between oxygen of the hydroxyl group of cholesterol molecules and hydrogen of the *CH* group in the lipid glycerol fragment. (A,C): RDFs in the whole range of distances; (B,D): Same RDFs in a short range of distances.

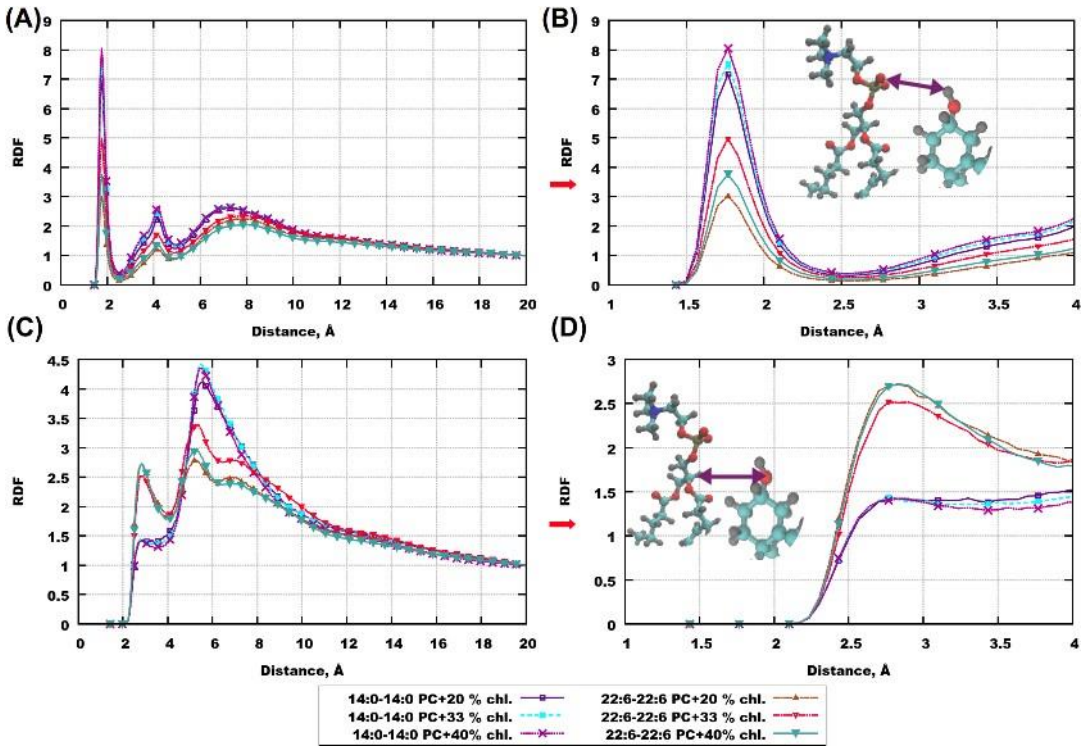

Figure S14: RDFs between cholesterol molecules and lipids for 14:0-14:0 PC and 22:6-22:6 PC bilayers with varying cholesterol content. (A,B): RDF between oxygen of the hydroxyl group of cholesterol molecules and oxygen of the phosphate group of lipid head; (C,D): RDF between oxygen of the hydroxyl group of cholesterol molecules and hydrogen of the *CH* group in the lipid glycerol fragment. (A,C): RDFs in the whole range of distances; (B,D): Same RDFs in a short range of distances.

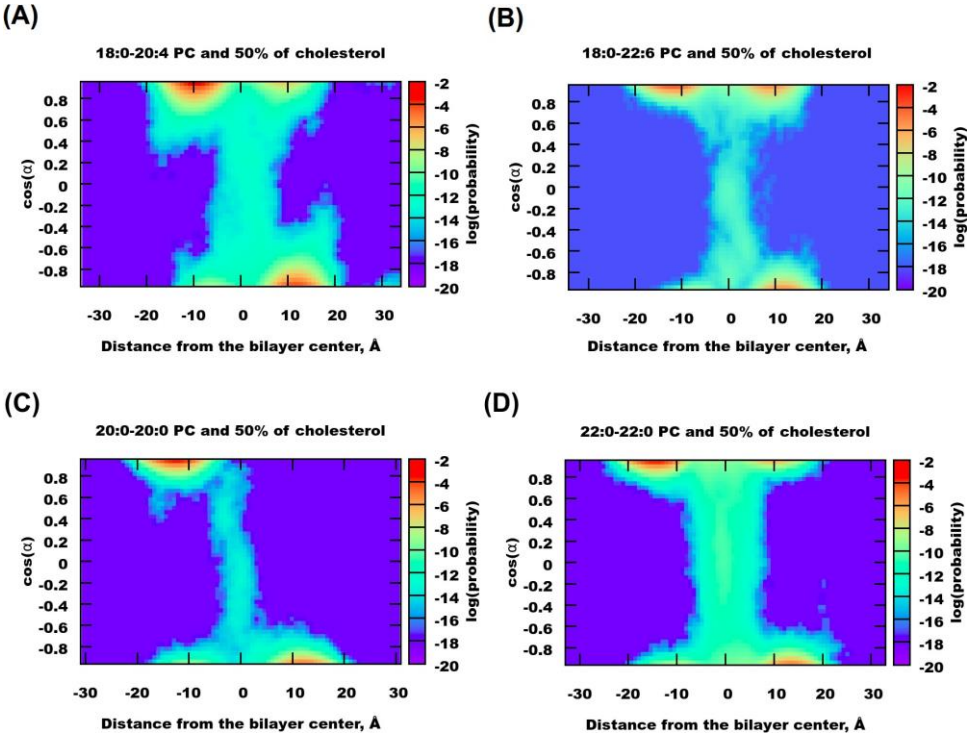

Figure S15: Density maps showing distribution of cholesterol as a function of its distance to the membrane middle plane and orientation, for selected bilayers containing 50 % *mol* of cholesterol.

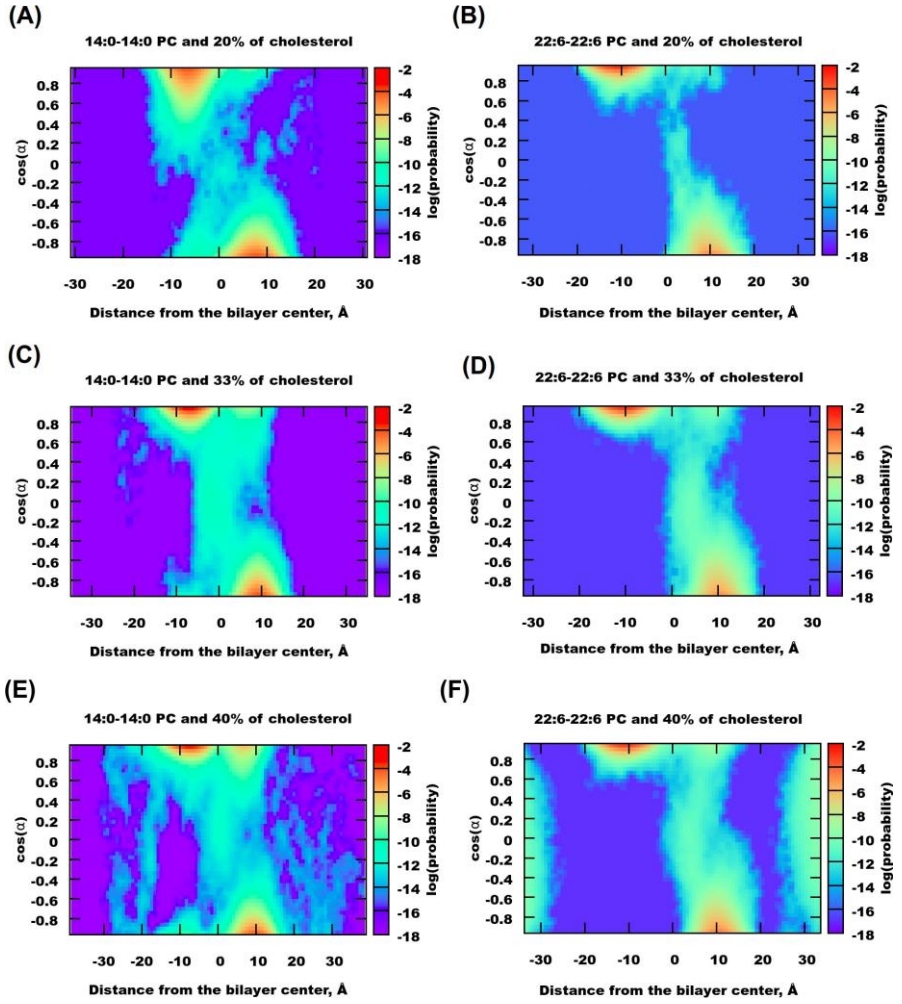

Figure S16: Density maps showing distribution of cholesterol as a function of its distance to the membrane middle plane and orientation, for 14:0-14:0 PC and 22:6-22:6 PC bilayers with varying cholesterol content.

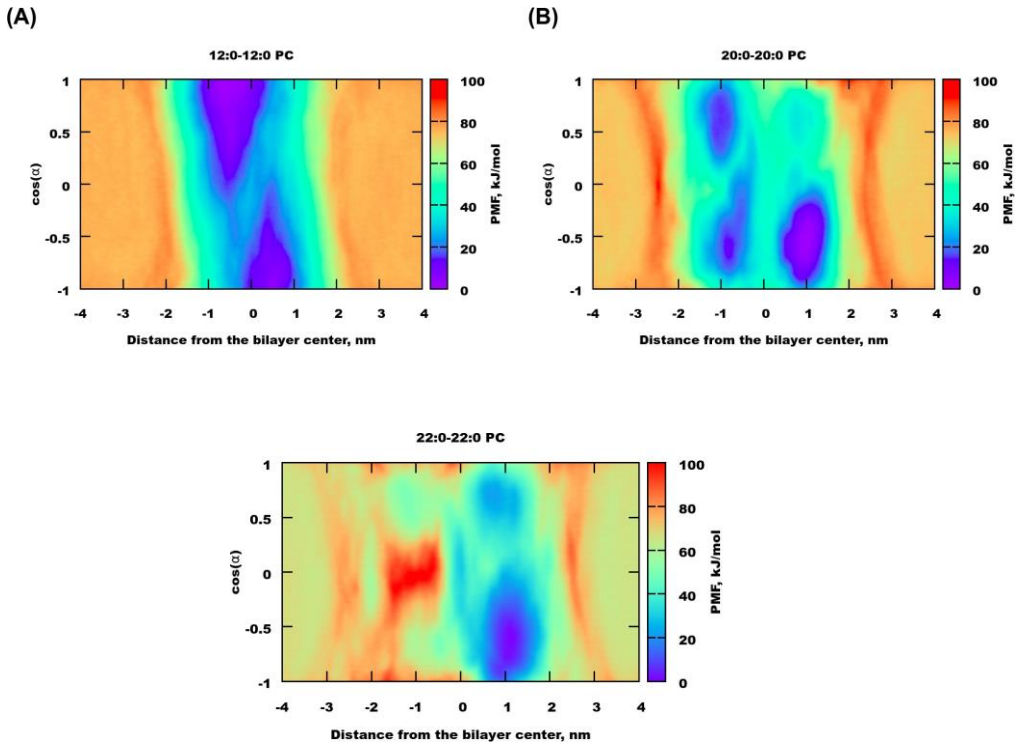

Figure S17: 2D free energy maps for selected bilayers (12:0-12:0 PC, 20:0-20:0 PC, and 22:0-22:0 PC)

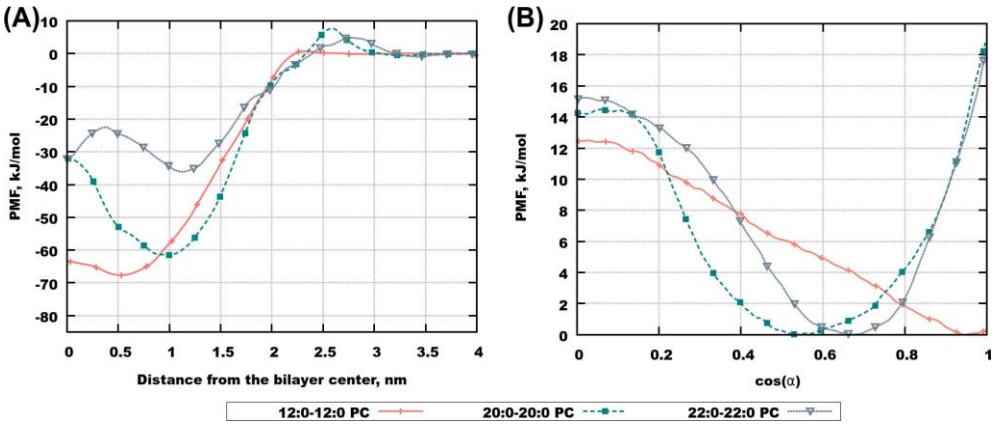

Figure S18: Free energy profiles for selected lipid bilayers integrated over one of the two collective variable. (A) Free energy profiles (Potential of mean force, PMF) as a function of positions of cholesterol molecules relative to bilayer center (B) Free energy profile as a function of orientation of cholesterol molecules.

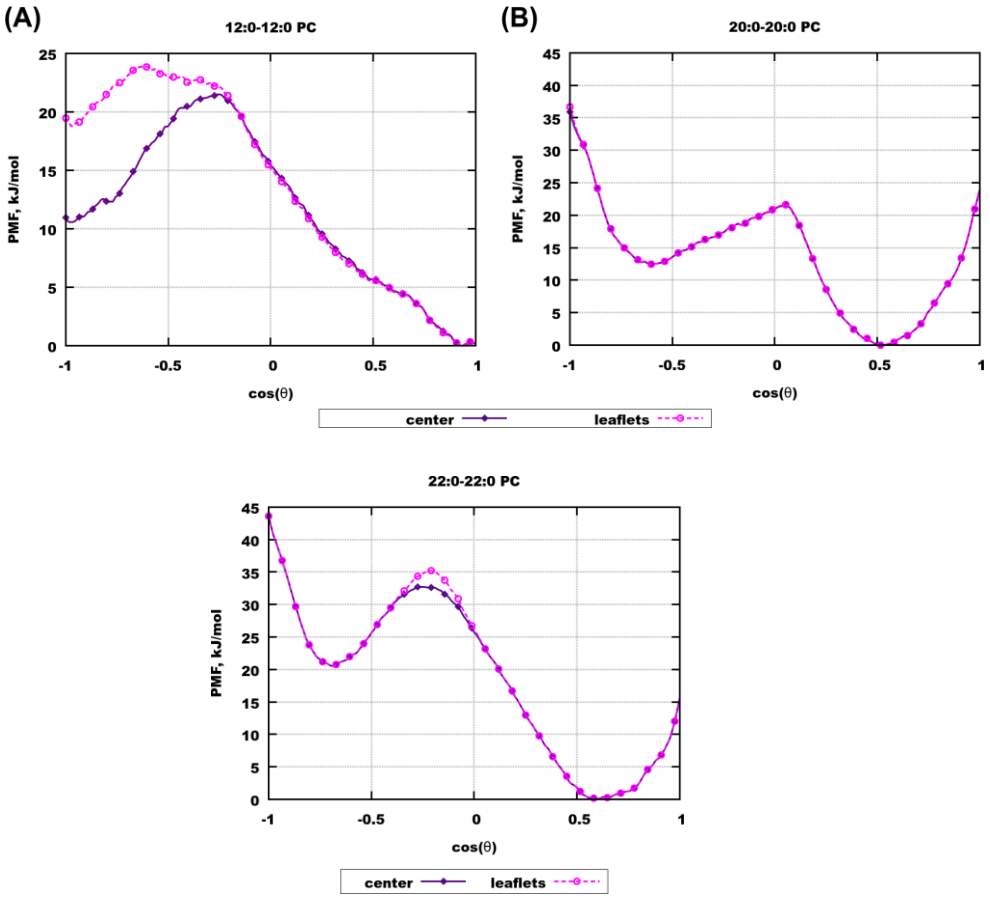

Figure S19: Relative orientational free energy profiles for selected bilayers. "center" - for cholesterol located within 3$\mathring{A}$ from the bilayer center; "leaflets" - for cholesterol within leaflets $[-1.5; -0.3]$ nm and for the lower layer $[0.3; 1.5]$ nm. Angle θ is defined as: $\theta = \alpha$ if z coordinate of the center of the mass of cholesterol molecule is positive (cholesterol in the upper monolayer), and $\theta = 180^{\circ} - \alpha$ if the coordinate z is negative (cholesterol in the lower monolayer)

Convergence of Metadynamics Simulations

Convergence of each MetaD simulation was evaluated from observation of three properties:

i) Evolution of the collective variables.

In a converged simulation, the system must sample the whole range of interest for the collective variables in a more or less uniform manner. For the first collective variable (distance from the bilayer center, CV1) the data are shown in Figures S18. One can see that CV1 samples relatively well the whole range of distances, with repeated motion of cholesterol between lipid and water phases on a sub-microsecond time scale and with somewhat worse performance for gel-type bilayers 20:0-20:0 and 22:0-22:0. The reorientational motion, presented by collective variable CV2, is much faster, as it is illustrated in Figure S19.

ii) Evolution of the computed PMF profile.

For each of collective variables, we choose a point of free energy minimum, and analysed changes of accumulated PMF in this point by comparison of PMF in the given time moment with the previous value taken 20 ns earlier. It is expected that these changes gradually decrease to zero. The data on convergence of the free energy profile for all considered bilayers are shown in Figure S20-S22.

iii) Evolution of Gaussians heights.

In well-tempered Metadynamics, the heights of added Gaussians are systematically decreasing during the course of simulations, thus removing the effect of the changing potential bias on the computed results. However sometimes the heights can temporarily increase if the system visits states which were seldom visited in the previous evolution and thus have a low value of the accumulated bias. Figures S23-S25 shows evolution of Gausian heights for the considered bilayers extracted from files ”HILLS” of the Plumed software.

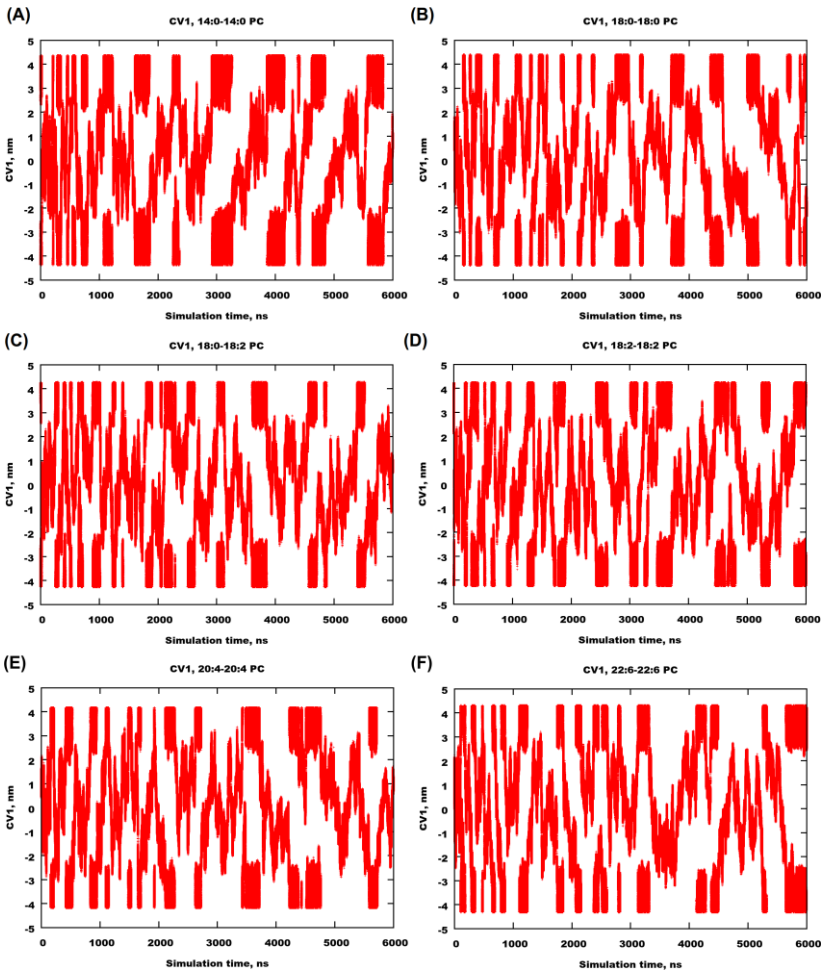

Figure S20: Evolution of the first collective variable CV1 (difference in z-coordinate between cholesterol and bilayer center of masses)

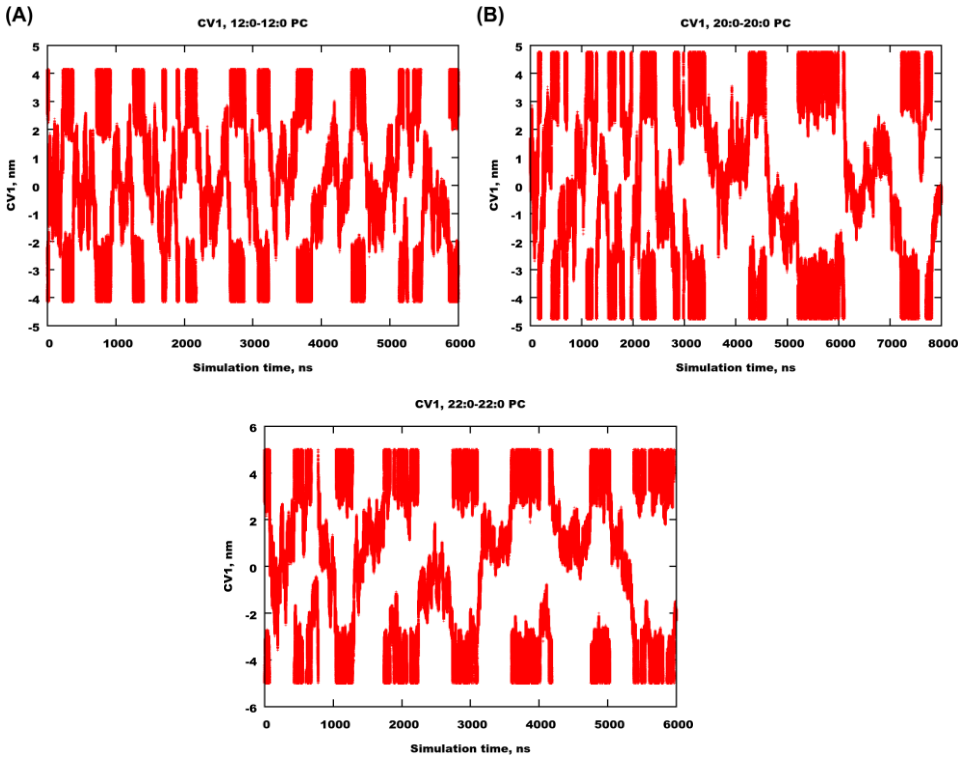

Figure S20, continuation: Evolution of the first collective variable CV1 (difference in z-coordinate between cholesterol and bilayer center of masses)

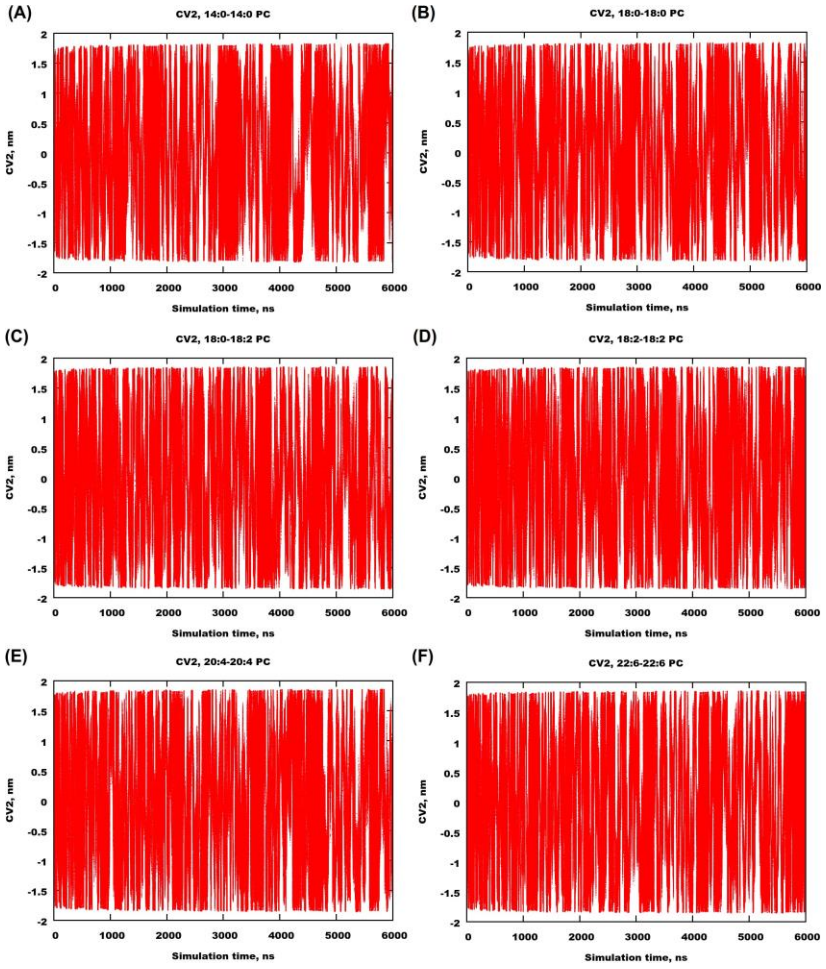

Figure S21: Evolution of the second collective variable CV2 (difference in z-projection of a vector between cholesterol O and C atoms)

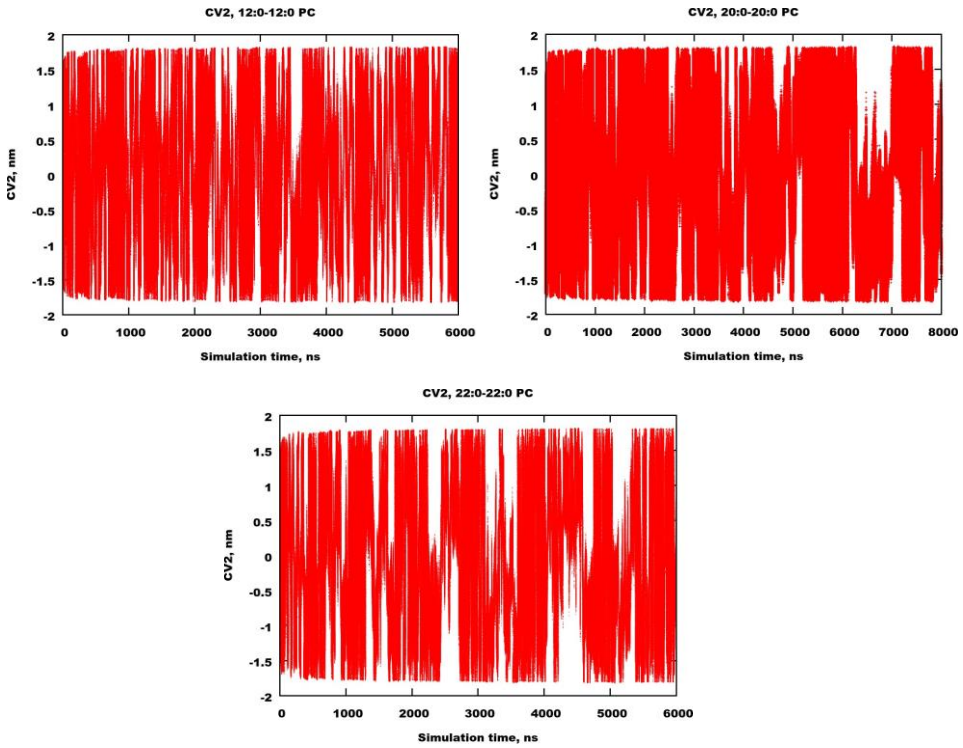

Figure S21, continuation: Evolution of the second collective variable CV2 (difference in z-projection of a vector between cholesterol O and C atoms)

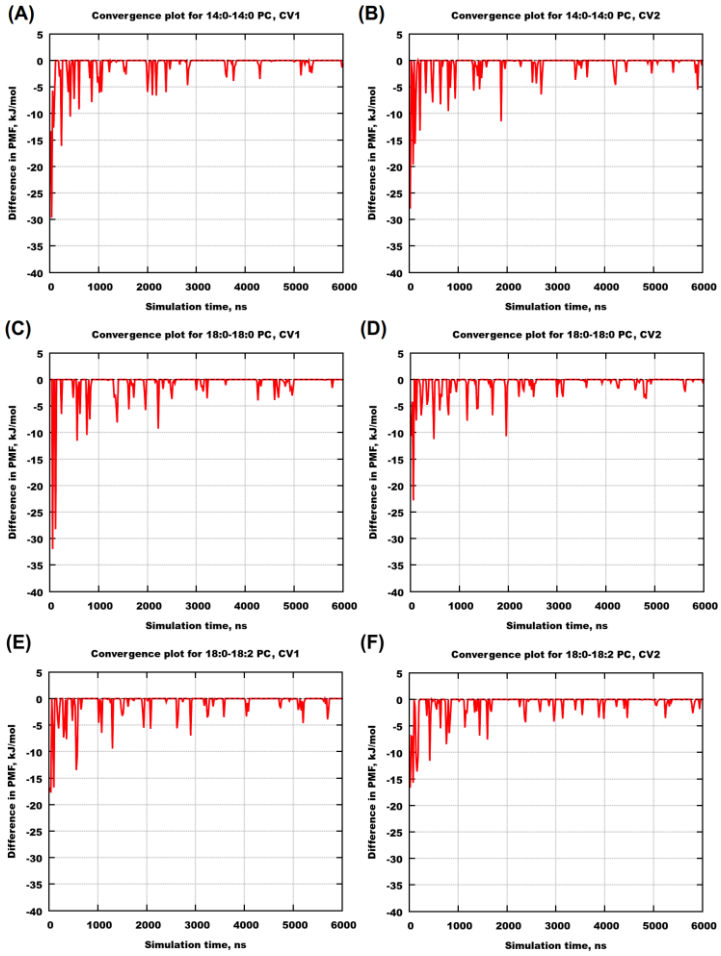

Figure S22: Convergence plots for selected bilayers. (A),(C),(E) Profiles for the collective variable 1. (B),(D),(F) Profiles for the collective variable 2. Every profile represents the evolution of a difference in PMF for a chosen local minima in time and was taken every 20 *ns*.

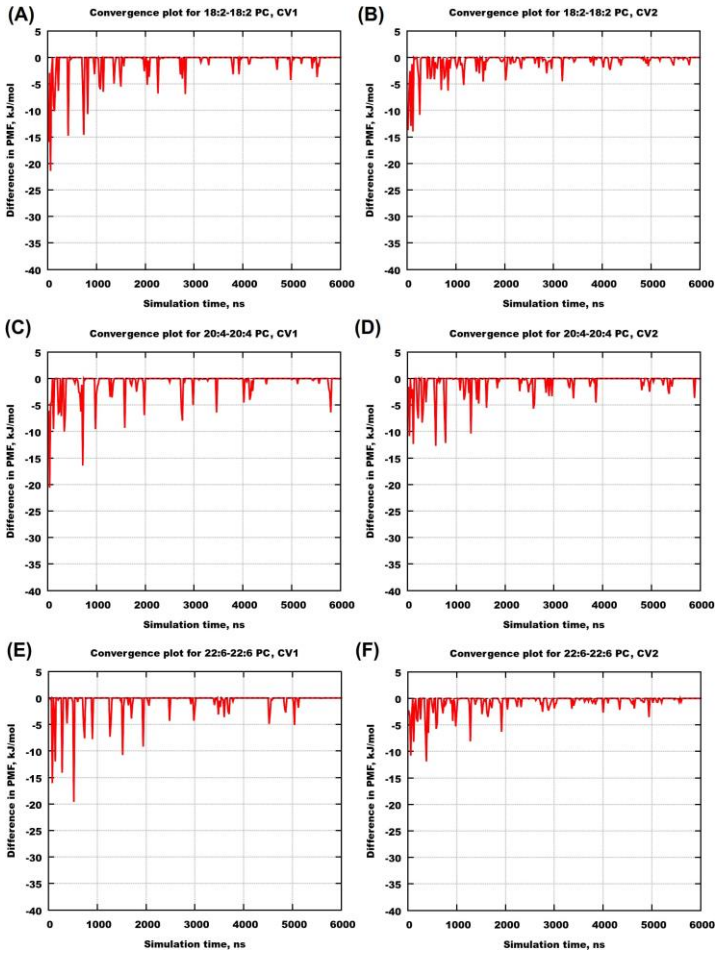

Figure S23: Convergence plots for selected bilayers. (A),(C),(E) Profiles for the collective variable 1. (B),(D),(F) Profiles for the collective variable 2. Every profile represents the evolution of a difference in PMF for a chosen local minima in time and was taken every 20 *ns*.

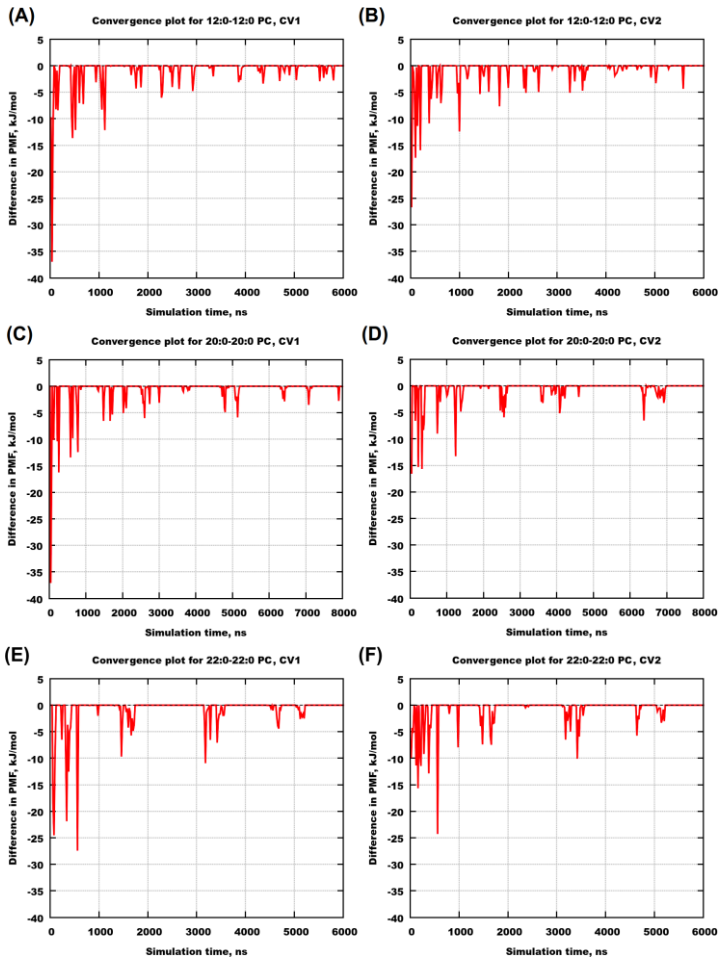

Figure S24: Convergence plots for selected bilayers. (A),(C),(E) Profiles for the collective variable 1. (B),(D),(F) Profiles for the collective variable 2. Every profile represents the evolution of a difference in PMF for a chosen local minima in time and was taken every 20 *ns*.

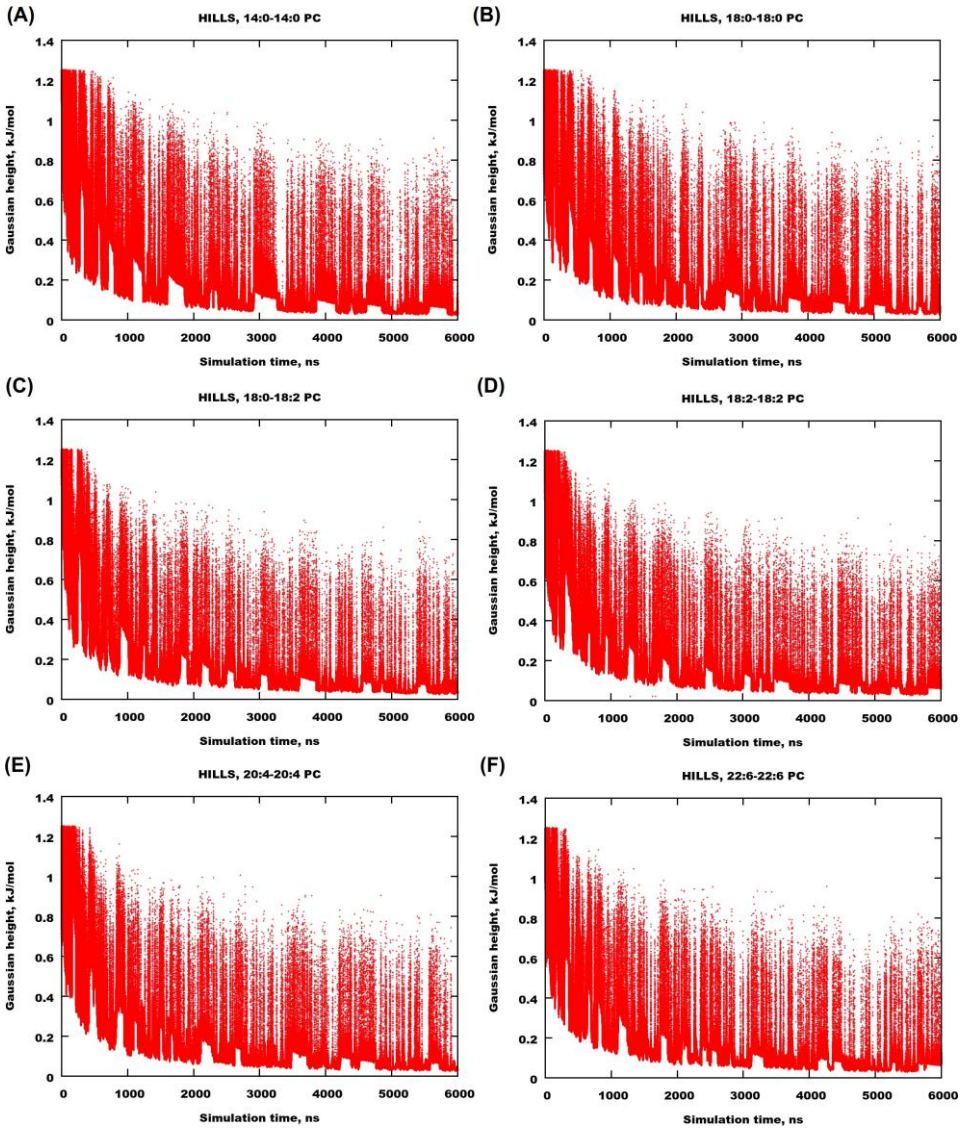

Figure S25: Gaussian heights from *HILLS*-files

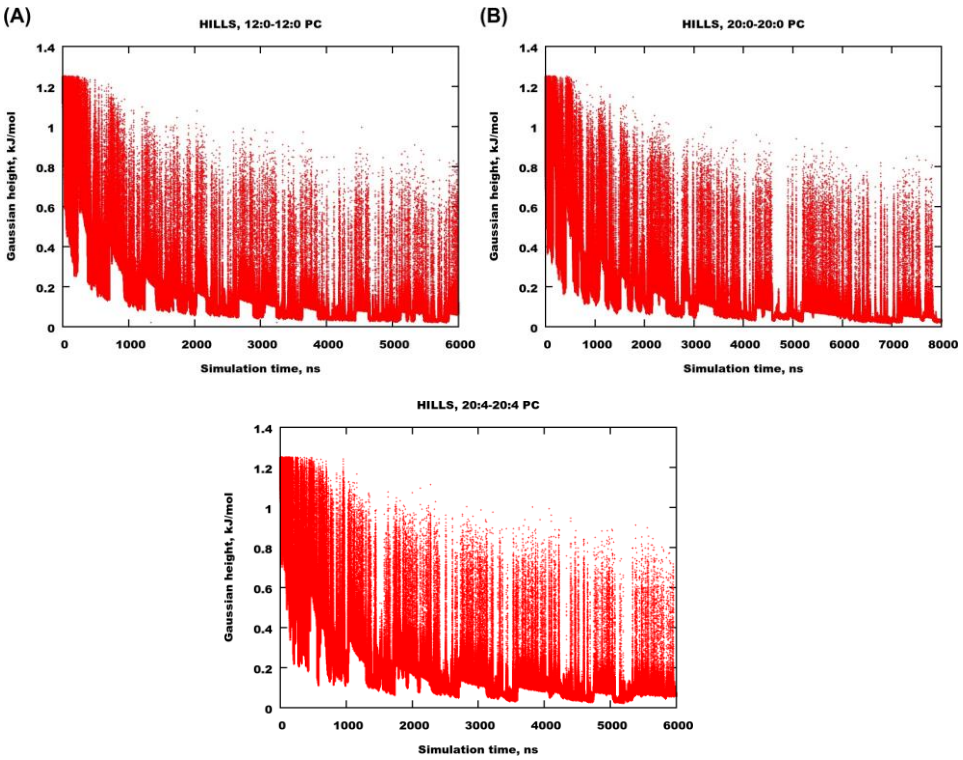

Figure S26: Gaussian heights from *HILLS*-files